IEEE Access
Multidisciplinary | Rapid Review | Open Access Journal

Received January 16, 2019, accepted February 22, 2019, date of publication March 7, 2019, date of current version March 26, 2019.

Digital Object Identifier 10.1109/ACCESS.2019.2903405

Spatial Characterization of Personal RF-EMF Exposure in Public Transportation Buses

MIKEL CELAYA-ECHARRI[1], (Student Member, IEEE), LEYRE AZPILICUETA[1], (Member, IEEE), PEIO LOPEZ-ITURRI[2,3], (Member, IEEE), ERIK AGUIRRE[2], SILVIA DE MIGUEL-BILBAO[4], VICTORIA RAMOS[4], (Senior Member, IEEE), AND FRANCISCO FALCONE[2,3], (Senior Member, IEEE)

[1]School of Engineering and Sciences, Tecnologico de Monterrey, Monterrey 64849, Mexico
[2]Electric, Electronic and Communication Engineering Department, Public University of Navarre, 31006 Pamplona, Spain
[3]Institute of Smart Cities, Public University of Navarre, 31006 Pamplona, Spain
[4]Telemedicine and eHealth Research Unit, Health Institute Carlos III, 28020 Madrid, Spain

Corresponding author: Leyre Azpilicueta (leyre.azpilicueta@tec.mx)

This work was supported in part by the School of Engineering and Sciences and in part by the Telecommunications Research Group of Tecnologico de Monterrey.

ABSTRACT New services and applications within vehicular environments employ multiple wireless communication systems, within a heterogeneous network framework. In this context, evaluation of electromagnetic field impact is compulsory in order to warrant compliance with current exposure limits. In this paper, E-field strength distribution within urban transportation buses is studied, in which different types of buses, as well as network configurations, are considered. E-field estimations are obtained within the complete interior volume of the urban buses, considering all the characteristics in terms of bus structure and materials employed, by means of an in-house-developed deterministic 3D ray-launching (3D-RL) code. In this way, relevant phenomena in terms of electromagnetic propagation and interaction are considered, such as multipath propagation and shadowing, which determine exposure levels as a function of transceiver location within the bus scenarios. The behavior in terms of E-field distribution of wireless public land mobile communication systems within transportation buses have been analyzed by means of measurement campaigns employing personal exposimeter devices. In addition, E-field volumetric distributions by means of 3D-RL simulations have been obtained as a function of user distribution within the buses, with the aim of analyzing the impact of user presence within complex intra-vehicular indoor scenarios, such as urban transportation buses. A comparison with current exposure limits given by currently adopted standards is obtained, showing that E-field levels were below the aforementioned limits. The use of deterministic simulation techniques based on 3D-RL enables E-field exposure analysis in complex indoor scenarios, offering an optimized balance between accuracy and computational cost. These results and the proposed simulation methodology can aid in an adequate assessment of human exposure to non-ionizing radiofrequency fields in public transportation buses, considering the impact of the morphology and the topology of vehicles, for current as well as for future wireless technologies and exposure limits.

INDEX TERMS Radiofrequency electromagnetic fields (RF-EMF), personal exposimeter (PEM), electromagnetic safety, E-field strength distribution, 3D ray launching (3D-RL), urban transportation buses.

I. INTRODUCTION

The use of public transportation systems has increased in the last years, particularly in the case of buses in urban scenarios. According the Eurostat's passenger transport statistics [1], the relative importance of the use of passenger transport by motor coaches, buses and trolley buses at European Union (EU-28) level was quite stable between 2004 and 2014, totaling approximately 9% of passenger transport modes. In the context of Smart Cities/Smart Regions, Intelligent Transportation Systems (ITS) play a key role in resource optimization as well as in improving user quality of experience. Within ITS service, heterogeneous wireless network operation is pivotal in order to provide context-awareness, inherently increasing the use of wireless systems in these scenarios. ITS systems are, unavoidably, sources of electric and

The associate editor coordinating the review of this manuscript and approving it for publication was Vittorio Degli-Esposti.

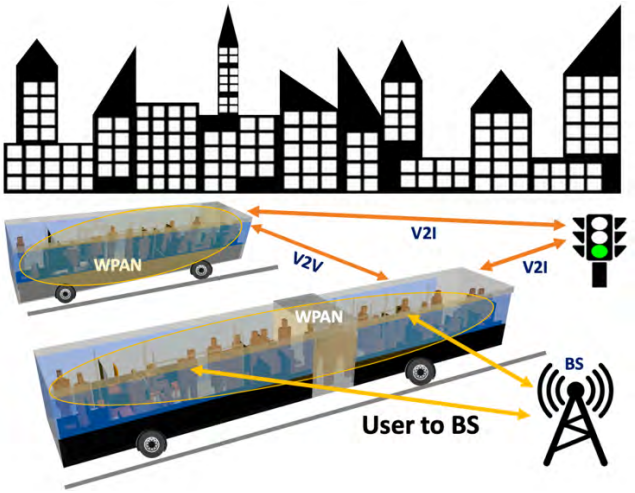

FIGURE 1. Schematic of vehicular communication systems: V2V, V2I, user communications. This work is focus on User to BS links as mobile phones are the main source of electromagnetic field for human exposure.

magnetic fields, to which a large proportion of the population is exposed. Hence, investigation of the effects of exposure of the general and occupational public to electromagnetic fields in transportation system is critically important, because these scenarios can be affected by different sources of EMF exposure, such as passengers' personal communications, communication systems that provide coverage inside the vehicles, vehicular communications (Vehicle to Vehicle V2V and/or Vehicle to Infrastructure V2I), and exposure due to external sources present in urban environments. Moreover, this impact will increase in large urban areas, owing to larger user densities and consequently more intensive use of urban transportation systems, as well as the greater deployment of wireless communication systems.

In general, wireless technologies in vehicular communications can range from short distance communications systems (RFID, WiFi, ZigBee, etc.) [2], which are normally used as Real Time Location Systems (RTLS) and to collect traffic data in order to inform users about the expected waiting time or the occurrence of incidences, to long range communications systems, such as UHF television signal, mobile technologies (UMTS, GSM, HSPA, LTE) or location systems like GPS [3] or GLONASS. In the near future, 5G communication systems will also be present, both in sub 6GHz frequency bands as well as on millimeter wave bands in order to provide low latency and high-speed communication capabilities. Fig. 1 presents a schematic view of different kind of vehicular communication systems that can be involved in urban environments. This work is focus on users to base station communication links (up-link).

Transport systems such as urban transportation buses are complex indoor micro environments in terms of wireless system operation and RF-EMF exposure, exhibiting specific radio wave propagation characteristics [4], with the largest RF-EMF field strengths attributed to mobile-phone use [5]. This exposure is caused by several factors [6]:

(1) The mobility of the bus, which can force the mobile phone to repeatedly connect to a different base station (umbrella cell/macrocell) (i.e., a handover), which can lead to transmit power variations.

(2) The structure of the bus, with the presence of metal elements and multiple scatterers, can increase transmit power levels of mobile devices, as compared to their use in exterior environments.

(3) The large amount of people confined in a small environment, increasing the chances of mobile-phone use, and thus reinforcing the aforementioned factors.

Taking into account the popularity and widespread use of transportation buses and their specific electromagnetic propagation characteristics, where several wireless technologies coexist, it's compulsory to analyze in-depth non-ionizing radiation exposure in this type of urban environment and verify compliance with legal exposure limits. As the main source of electromagnetic field for human exposure is the mobile phone, in this work, a complete E-field strength distribution study, focusing on mobile communication technologies, is carried out considering the usual E-Field exposure levels in real transportation bus routes. Simulations have been performed by means of an in-house 3D-RL algorithm. In addition, a dynamic approach has been implemented with the use of a PEM to monitor EMF exposure in a rigid and articulated bus along two different routes, showing accordance with simulation results. It must be pointed out that considering the very low exposure levels and research results collected to date, there is no convincing scientific evidence that the weak RF signals from wireless networks or base stations can cause adverse health effects. Nevertheless, research is still being promoted by WHO [5] to determine whether there are any health consequences from the higher RF exposures levels.

Several works have studied the human exposure to EMF in public transport systems, such as cars, airplanes, and subways [7]–[9]. In these environments, electromagnetic fields exposure presents particular features, given by the fact that individual exposure levels can be affected by the emission from personal communication devices of nearby users. Reference [10] evaluates the absorption in a train environment. The work compares GSM and UMTS exposure and concludes that the UMTS femtocell installation in this environment drastically reduces the total absorption, making other users' contributions to total absorption negligible. The work in [9] presents a mobile network service on a train through a miniature mobile-phone base station or small cell in order to improve coverage and capacity. Moreover, brain exposure of the user could realistically be reduced by a factor 35 and the whole-body exposure by a factor 11. In recent years, the study and analysis of magnetic fields have notoriously increased due to the development of hybrid vehicles, which have generated a relevant contribution to the total exposure. Electric and hybrid vehicles give rise to particular concerns because they use currents and voltages that are much higher than those used in conventional vehicles, and which can therefore potentially generate much

higher intensity fields. However, comparison of electromagnetic field levels from different modes of transport concluded that there was no major difference in fields between electric vehicles and conventional vehicles [11], [12].

Although several works have been presented in different transportation systems (cars, airplanes, metro subways, trains), for the author's knowledge, there isn't a specific study of EMF exposure in public transportation buses. In [4], the electromagnetic propagation characterization inside the buses is presented, showing that these types of vehicles exhibit unique characteristics related with radio wave propagation. These particular features of the environment make necessary the assessment of emissions produced by different wireless communication technologies in these types of vehicles, due to the fact that user density variations can lead to different distributions of RF power and hence, variations in overall exposure levels.

This work is organized as follows: in Section II, the current legislation regarding the non-ionizing radiation exposure for different countries is presented. In Section III, the implemented campaign of measurements in the different urban routes with the PEM is explained, as well as the in-house deterministic methodology used for simulation of the two models of real urban buses where different wireless technologies, transmission frequencies, transmission positions, and user densities, have been considered. Section IV presents the simulation and measurements results for the different buses, and discussion in relation with different exposure level thresholds, showing that for all cases, E-Field results are below the maximum reference levels of ICNIRP. In consequence, a simulation-based analysis methodology is provided, aiding in the assessment of future wireless deployments. Conclusions are presented in Section V.

II. LEGISLATION

The publication of the European recommendation 1999/519/EC allowed a harmonized vision of the protection of health against non-ionizing radiation in all the European Union [13]. The recommendations are based on the Guidelines from the International Commission on Non-Ionizing Radiation Protection (ICNIRP) [14] which are recognized by the World Health Organization (WHO) [15] and by the International Labour Organization (ILO).

Limits for general public and worker exposure are different in the ICNIRP recommendation. The main difference is based on the fact that workers are exposed under known conditions, they are aware of the RF emissions and trained to take appropriate precautions, while the general public comprises individuals of all ages and of varying health status and may include particularly susceptible groups of individuals. In addition, general public may not be aware of the presence of the RF emissions. In the high-frequency range 10 MHz-10 GHz, the general reference levels for electric and magnetic fields are lower by a factor of 2.2 than those set for occupational exposure. The factor 2.2 corresponds to the square root of 5, which is the safety factor between

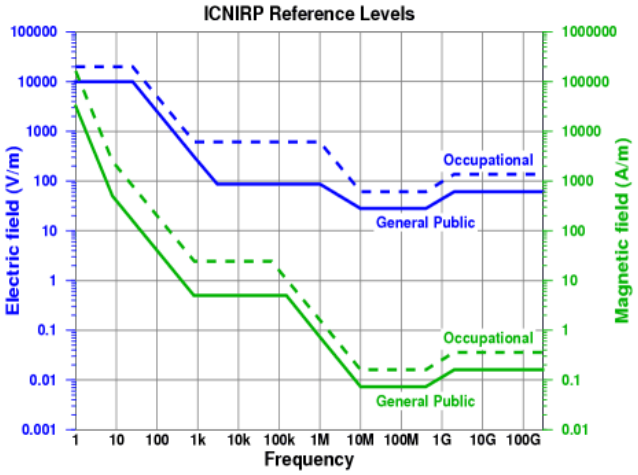

FIGURE 2. ICNIRP reference levels for electric and magnetic field for occupational and general public radiation exposure with the frequency dependency.

the basic restrictions for occupational exposure and those for general public exposure. Fig. 2 shows the exposure limits for electric and magnetic fields, for occupational and general public exposure, published by ICNIRP.

Exposure limits in different countries vary by factors of 10 or more, depending on the frequency range and the type of public exposure: occupational (workers) or the general public. The difference between regulatory frameworks on RF exposures are based on different factors, starting from precautionary principle application [16]–[18] and involving specific and local socio-political contests [19].

Most countries follow the ICNIRP recommendations for limiting exposure to RF fields. However, some differences exist between North America, Eastern Europe and Western Europe [20], [21]. Regulations in EU countries are based on the adoption of at least three different approaches [22], as shown in Table 1.

There are clear differences between exposure limits in Eastern Europe (EE) countries (Russia, Hungary, Bulgaria, Poland, Czech Republic, among others) and Western countries, referring to the over 50 countries that have adopted the rules of ICNIRP [14] and the American standard of IEEE C95.7 [23].

Safety standards of Western countries protect against known and acute biological effects and thermal effects, which normally are compensated by the human body defense mechanisms (sweating, heart beating increasing), but that can become dangerous if electromagnetic field levels are so high as to defeat the human body compensation mechanisms. The basic restrictions are defined in terms of Specific Absorption Rate (SAR). In contrast, the rules termed as "hygiene" (hygienic standards) in the countries of EE aim to protect against non-thermal effects that may be caused by the chronic and continuous exposure over time at low levels of exposure. The basic restriction is a parameter called power load defined as the product of the field intensity and the duration of exposure [14], [24]. Another feature of the EE countries is the

TABLE 1. Different regulatory approaches by EU countries.

Group	Countries	Regulations	National RF Limits	Basis
G1	Cyprus, Czech Republic, Estonia, Finland, France, Hungary, Ireland, Malta, Portugal, Romania, and Spain	Mandatory. Identical to EU Directive 2013/35/CE	Based on ICNIRP reference levels	As ICNIRP, science-based
G2	Austria, Denmark, Latvia, Netherlands, Sweden, UK	No binding regulations	Recommended limits based on ICNIRP reference levels but not mandatory	As ICNIRP, science-based
G3	Belgium,	Mandatory.	Inferior to	Precautionary
	Bulgaria, Greece, Italy, Lithuania, Luxembourg, Poland, Slovenia	More stringent rules than EU Directive	ICNIRP reference levels	principle, socio-political factors

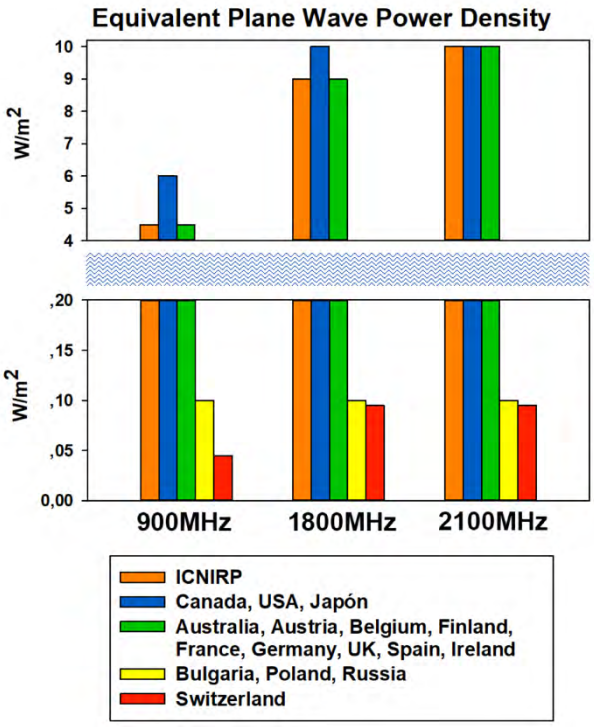

FIGURE 3. RF exposure limits for the general public in different countries. Equivalent plane wave power density, W/m^2.

dose concept, defined as the limitation of exposure duration to EMF cumulatively. It is calculated by multiplying the duration of exposure by 2W/m^2, with a limit of up to 8 hours in the case of occupational public. For the general public, a similar formula is applied but with a time limit of 24 hours of exposure [25]. In general, the exposure thresholds in EE countries (Bulgaria, Poland, Romania and Slovakia) are far lower than in the countries of Western Europe. Moreover, the approach to the protection, and in particular, the parameters used when setting exposure limits, are different from those used in other international standards in Western countries [26]. They could also be attributed to differences in the stages of development of regulations and standards, such as the methodology used in experimental studies, different philosophies for the development of standards, the scientific data used as a basis for standards, or differences in risk perception.

In relation with regulations in the rest of the world, the safety standards are based on the European or American recommendations: ICNIRP [14] and ANSI / IEEE C95.7 [23]. The exception is Australia, where in 2002, the Australian Radioprotection and Nuclear safety Agency (ARPANSA) published its own standard entitled Radiation Protection Standard - Maximum Exposure Levels to Radiofrequency Fields - 3 kHz to 300 GHz [27], where the specified limits are based on the ICNIRP 1998 Guidelines. In Fig. 3 RF exposure limits comparison for different world-countries is presented at different frequency bands.

The European Union adopted the reference exposure levels to time-varying EMFs proposed by ICNIRP for both the general public and workers. This initiative had a positive effect and most countries transposed this Recommendation in its legislation. In Spain the publication of the RD 1066/2001 [28] involved the incorporation of the Recommendation 1999/519/EC to the legal system, and filled a gap in legislation that served to address community concerns about the health consequences of RF-EMF exposure.

For what concerns professional exposures, in 2013, the European Parliament and the Council of the European Union issued the Directive 2013/35/EU [29], which aims to address all direct and indirect biophysical effects of EMF, in order not only to ensure the health and safety of each worker, but also to create a minimum basis of protection for all workers in the Union. New international exposure limits are included, leaving some flexibility in the military sectors and areas of use of resonance imaging equipment, and forcing employers to establish assessment measures for risk reduction.

Transport systems are microenvironments where general and occupational exposure limits must be considered to verify the compliance of EMF exposure legislation. In the case of public transport systems, such as transportation buses, "occupational exposure" is applied to those individuals who are exposed to EMFs as a result of performing their regular job activities (i.e. bus driver). On the other hand, "general public exposure" is applied to all passengers of public transportation systems.

III. MATERIALS AND METHODS

A. MEASUREMENT CAMPAIGN

A measurement campaign was designed and implemented in two different urban transportation bus routes, to analyze the

TABLE 2. Measured frequency bands of the EME Spy 121 PEM.

Technology	Frequency (MHz)
FM	88 - 108
TV3	174 - 223
TETRA	380 - 400
TV4&5	470 - 830
GSM+UMTS 900 (UL)	880 - 915
GSM+UMTS 900 (DL)	925 - 960
GSM 1800 (UL)	1710 - 1785
GSM 1800 (DL)	1805 - 1880
DECT	1880 - 1900
UMTS 2100 (UL)	1920 - 1980
UMTS 2100 (DL)	2110 - 2170
WIFI 2G	2400 - 2500
WIIMax	3400 - 3800
WIFI 5G	5150 - 5850

different wireless technologies, specifically mobile phones as they are the main source of EMF to which passengers are exposed. The corresponding received E-field distribution levels has been obtained, thus, compliance with legal exposure thresholds can be assessed.

Recent works have evaluated the exposure levels in urban environments and dynamic conditions, employing personal exposimeters (PEM) [30], [31], typically used for measuring exposure to EMF in epidemiological studies, due to their small size and weight. There are different strategies and methodologies to monitor the EMF exposure in wide areas, such as urban environments. Specifically, it is possible to distinguish two types of procedures, static and dynamic [32]. Static methods are generally carried out with a spectrum analyzer to determine the contribution of a specific frequency band to the total E-field measured in a specific position. This method consumes considerable resources in terms of equipment, training and staff costs. On the other hand, broadband exposure assessment methods are very accurate for determining exposure at a specific point in time and space, but not in dynamic conditions over the time. In these cases, PEMs are devices that allow obtaining numerous measurements at different locations and with little effort.

The selected tool for this study is the EME Spy 121 personal dosimeter (SATIMO, Courtaboeuf, France, http://www.satimo.fr/), which is shown in Fig. 4. The EME Spy 121 is a portable measurement device which detects power flux density and electrical field strength over time. It has been configured to obtain an E-field sample every four seconds (lowest device possible setup) at frequency bands ranging from radio FM (frequency modulation; 88–108MHz) to WiFi 5G (5.1–5.8GHz). The measured frequency bands of the EME Spy 121 are summarized in Table 2.

The measurements have been performed in normal business days and respecting the usual routine of the bus.

FIGURE 4. EME Spy 121 personal dosimeter used for the campaign of measurements within the buses.

FIGURE 5. Different routes of the buses chosen for the measurement campaign in the city of Pamplona, Spain. (a) Line 4 with a rigid bus. (b) Line 6 with an articulated bus.

Fig. 5 shows both itineraries, which are part of the city of Pamplona (Spain) public transport system which is used every day by thousands of users.

One of the key elements in wireless system operation is the analysis of coverage/capacity relations, which are conditioned by overall interference levels. In this sense, user density is a relevant aspect in the determination of coverage/capacity values. Therefore, high and low population density areas have been considered, enabling inter-area data comparison. With this goal, the chosen bus lines start in suburbs, crosses the center of the city and ends in suburbs. The round trip was also evaluated.

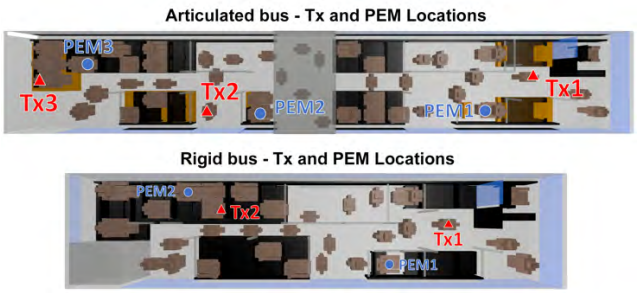

FIGURE 6. Transmitter and PEM locations scheme for the measurement campaign in the different urban transportation buses.

A single trip along the complete route of Line 4 has a duration of 45 minutes with a rigid bus, and a single trip along the route of Line 6 has a duration of 30 minutes with a metallic articulated bus. The main difference between the two types of buses is the length of each one, their different topology and morphology and the metallic bouncy structure in the center of the bus in the articulated one. Along the different routes of the buses, different mobile voice connections were performed by members of our group, emulating a passenger of the bus making a call. With this procedure, we were able to analyze different areas of the buses, measuring E-field levels in the closest area where the phone call was being made. For all cases, the PEM was located in the closest sitting place within an area of 2m around the user who was making the phone call, as it can be seen in Fig. 6. This approach was considered knowing that the highest EMF exposure levels were achieved when making a phone call in proximity to the terminal [33]. Moreover, this location was employed in order to measure the EMF exposure levels in the most probable location for another passenger within the bus. In addition, no other electronic devices, such as laptops, other phones or tablets were used during the data collection process, avoiding inaccurate or incorrect measurements. On the other hand, considering the structural differences of the two models of buses, different areas were chosen to perform the phone calls and analyze the corresponding E-field levels. Thus, the transmitter was located in three different locations in the articulated bus: in the front part of the bus in the central aisle, in the central part of the bus in a dedicated sitting area and in the rear part of the bus in another dedicated sitting area. For the rigid bus, the transmitter was located in two different positions: in the front part of the bus in the central aisle and in the rear part of the bus in a dedicated sitting area. Transmitter and PEM locations are depicted in Fig. 6. Measurement results and discussion are presented in Section IV.D.

B. RAY LAUNCHING TECHNIQUE

With the aim of analyzing non-ionizing radiation exposure for each passenger within the buses, an in-house 3D-RL technique has been used. The algorithm has been developed in Matlab programming environment and it has been widely tested [34] including transportation scenarios such as airplanes [35] or cars [36]. Other simulation approaches such as FDTD or other full wave methods [37] could have been employed, but the size of the bus and the consideration of all the elements inside it, considerably increase computational time. On the other hand, empirical simulation methods [38]–[40] reduce computational cost with lower accuracy. These techniques are unsuitable for complex scenarios, such as urban buses leading to high deviation in field estimations. Hence, 3D-RL techniques are the best option in this case, considering that they provide high accuracy, a Root Mean Square Error (RMSE) of 3-6 dB, an absolute mean error of 4-5 dB and Standard Deviation (SD) of 1-7 dB, with a low processing time [34], [41]–[44].

The 3D-RL algorithm is based on Geometrical Optics (GO) and Geometrical Theory of Diffraction (GTD) [45]. The main principle of the RL techniques is to identify a single point on the wave front of the radiated wave with a ray that propagates in space following a combination of optic and electromagnetic theories. It is performed three-dimensionally, with angular resolution (horizontal and vertical planes) in a predefined solid angle that considers the radiation diagram of the transceiver sources. Spatial resolution is also defined by a uniform hexahedral mesh. Parameters such as frequency of operation, antenna radiation patterns, maximum number of reflections until extinction, ray angular resolution, and cuboid dimensions are considered. Moreover, the material properties for all the elements within the scenario are considered, given the dielectric constant and the loss tangent at the frequency range of operation of the system under analysis. When a ray impacts with an obstacle, reflection, refraction and diffraction will occur, depending on the geometry and the electric properties of the object. The 3D-RL tool is based on a modular structure, where electromagnetic safety analysis has been implemented as a new module for non-ionizing radiation exposure analysis. In this library, once the power level results have been obtained for all the spatial points of the scenario, E-field results are obtained using equation (1) [46]:

$$P_R = \frac{E^2}{480\pi^2}\frac{c^2}{f^2}G_R \tag{1}$$

where P_R is the received power in Watt, E is the E-field level in V/m, $c = 3{*}10^8$ m/s is the light speed, f is the frequency under analysis and G_R is the receiver antenna gain.

The 3D-RL tool enables the inclusion of human body models in the scenario under analysis. These models have been implemented considering skin dielectric properties in a modular way and have been previously tested [47].

The proposed in-house developed 3D-RL algorithm gives a RMSE of 0.22-1.5 dB, an absolute mean error of 1-3 dB and a SD of 1-6 dB, when compare with real measurements, as presented in [34] and [48]. It must be pointed out that the RL approach provides an uncertainty near field results area in the vicinity of the transmitting antenna, which has not been considered in the presented work. Thus, an exclusion area of 1.2m (4λ for 900MHz frequency band) and 1m (6λ and

FIGURE 7. Real vehicles used in the campaign of measurements (left) and internal distribution of the articulated bus (right).

7λ for 1800 and 2100MHz frequency bands, respectively) around the transmitter has been considered in order to avoid near field results.

C. SCENARIO DESCRIPTION

Fig. 7 (left) shows the two types of urban buses employed for measurement tests: the articulated bus (top) and the rigid bus (bottom). The internal distribution of one of the articulated buses, with seats and handhold distribution can be seen in Fig. 7 (right). As it can be observed, the buses have two types of seats: the red ones, reserved for seniors, pregnant women, adults with children or individuals with disabilities, which have different dimensions or are prepared to engage wheelchairs or prams, and the turquoise blue seats, for the rest of the passengers. The main differences between the two types of buses is their length, their interior structure and the metallic bouncy structure in the center of the bus for the articulated ones.

The same scenarios of Fig. 7 have been implemented in the 3D-RL tool, considering in both cases all furnishings and the dielectric properties of the materials employed, considering not only the free space losses, but also other phenomena like reflection, diffraction or refraction. Since the ultimate aim of urban buses is the transportation of people and their influence in radio electric propagation is relevant owing to the dispersive characteristics of the human body, simplified human body models have been randomly introduced within the vehicles. In addition, not only the position of individuals has been varied, but also their density has been modified to evaluate their impact in EMF distribution according to their location and proximity to the transmitting antenna.

Fig. 8 depicts the six scenarios implemented along with the human body model densities considered for simulation. Low, medium and high-density conditions have been considered for both types of buses, which represent the 25%, 50% and

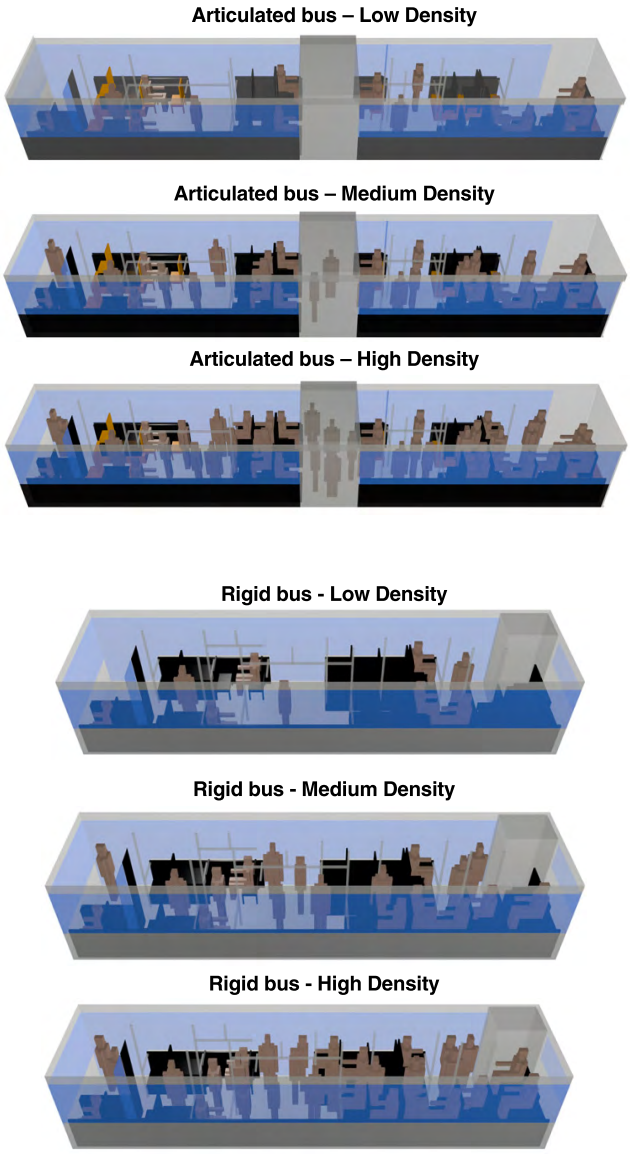

FIGURE 8. Articulated and rigid bus scenarios implemented for simulation with different indoor designs and passenger densities.

75% of the maximum capacity of passengers of the buses, respectively. The maximum capacity of passengers in the articulated bus has been considered to be 56 passengers, and in the rigid bus 39 passengers.

Different simulations have been performed emulating a mobile phone device making calls at the same positions inside the buses as the phone calls made in the measurement campaign. These simulations give results for E-field levels for the whole 3D scenario, which enable the comparison of the received E-field levels at the same spatial point as the measurements. The mobile phone frequency bands simulated have been GSM 900MHz, GSM 1800MHz and UMTS 2100MHz. The considered transmitted power for simulation follows the maximum and minimum transmitted power permitted for the different mobile frequency bands, shown in Table 3 [7]. Simulation results have been obtained

TABLE 3. Maximum and minimum transmission power for the different frequency bands.

Band name	Frequency band (MHz)	Maximum transmission power	Minimum transmission power
GSM 900	880-960	2W	3.16mW
GSM 1800	1710-1880	1W	1mW
UMTS 2100	1920-2170	125mW	12.6mW

TABLE 4. Parameters for the 3D-RL simulations.

Simulation Selected Parameters		Ref.
Frequency of operation (MHz)	900 / 1800 / 2100	
Transmitted power level	See Table 2.	
Tx / Rx Gain	0 dB	
Horizontal angular resolution ($\Delta\Phi$)	π/180 rad	[45]
Vertical angular resolution ($\Delta\theta$)	π/180 rad	[45]
Permitted maximum reflections	6	[45]
Angular resolution Diffracted rays	π/20 rad	[49]
Cuboids size	10cm	

considering maximum transmission power, in order to provide assessment in worst case scenarios.

The rest of the simulation input parameters employed in the scenarios under analysis, are shown in Table 4.

IV. RESULTS AND DISCUSSION

A. HUMAN BEINGS DENSITY COMPARISON

As stated above, the comparison of E-field exposure levels as a function of user distribution within both type of urban buses, has been obtained. Simulations have been performed for the articulated and rigid bus, with the maximum transmitted power per frequency band, to assess the highest E-field exposure level distribution within the scenarios.

Fig. 9 shows the comparison of the articulated bus E-field exposure levels for the three different human body model density values, in the GSM 900MHz frequency band. The transmitter antenna has been placed at the location X = 1.18m, Y = 2.49m, Z = 1.1m, emulating a standing passenger making a hands-free phone call in the front part of the bus.

The E-field exposure levels vary from very low values close to zero in far areas from the transmitter location, to higher values, around 30V/m, showing the most remarkable values in the transmitter close range (2m-2.5m radius). This E-field exposure trend increases as a higher user distribution is considered. This pattern is the result of the body shielding created by the passengers located close to the emitting device, which block and concentrate the signal in the front part of the vehicle. On the other hand, for the low-density case, E-field exposure levels exhibit a more homogeneous distribution along the complete volume of the scenario, due to a decrease of obstacles (i.e., lower passenger densities

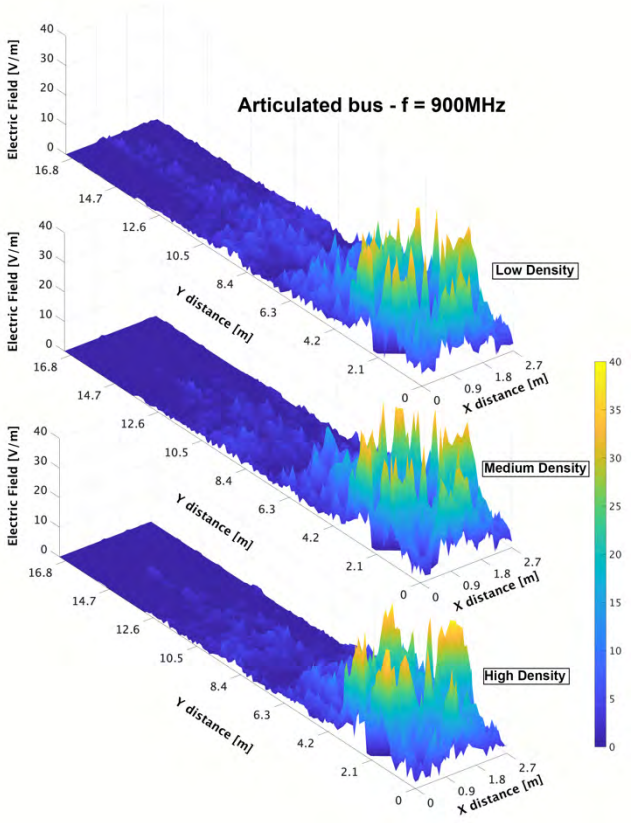

FIGURE 9. Comparison of the simulated E-field exposure levels within the articulated bus at GSM 900. The transmitter is placed in the front of the bus with the maximum allowed transmitting power. 4λ m exclusion area around the transmitter has been considered in order to avoid near field results.

equal better signal propagation in open spaces due to lower shadowing). Hence, a relevant increase in E-field average levels is obtained especially, in the central aisle of the bus. In Fig. 10, the same comparison is depicted for the rigid bus for the GSM 1800 frequency band. In this case, the transmitter has been placed at X = 1.9m, Y = 8.75m, Z = 1.3m, emulating a sitting passenger making a phone call in the rear part of the bus.

Although the maximum transmitted power for this frequency band is lower (1W in contrast with 2W for the previous case), higher E-field exposure values are obtained for the rigid bus cases. However, for both types, the highest exposure levels are in compliance with current EMF exposure limits, as it is presented in Section IV.C. As in the articulated bus case, the same signal propagation pattern and E-field exposure trend is obtained for the rigid bus case, but with a higher impact in the vicinity of the transmitter. The high-density case presents the highest E-field exposure distribution in the vicinity of the emitting antenna (1.5m radius). These effects are generated by a combination of the body shielding created by the passengers surrounding the transmitter location and a non-open transmitter location, placed in a dedicated sitting area in the rear part of the bus. As expected, a decrease in the number of obstacles within the bus, along with a shorter

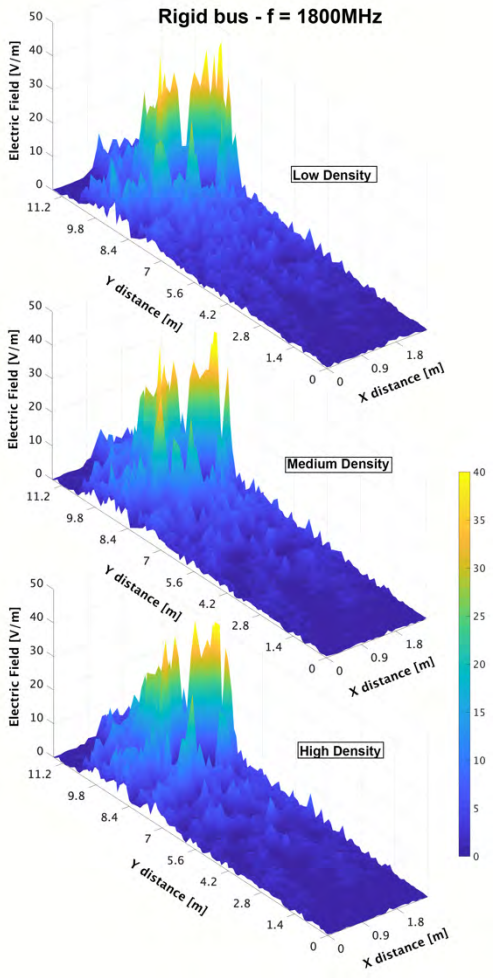

FIGURE 10. Comparison of the simulated E-field exposure levels within the rigid bus at GSM 1800. Transmitter placed in the rear part of the bus with the maximum allowed transmitting power. 6λ m exclusion area around the transmitter has been considered in order to avoid near field results.

length of the vehicle, results in higher E-field exposure levels for the three user density cases considered.

In order to provide clear insight in relation with E-field behavior within the bus scenarios, Table 5 presents the E-field average values for the different impact areas, considering concentric rings surrounding the transmitter antenna ranging from 1m to 4m radius (near field results have been excluded).

The different concentric rings impact areas are presented in Fig. 11, depicted with different colors. These colors match with the rows of Table 5.

For the articulated bus case, the highest exposure E-field values are concentrated in an area delimited by 2m-2.5m radius from the transmitter location. On the other hand, for the rigid bus case, a smaller impact area is observed (1.5m radius) due to the presence of multiple users close to the emitting device, and its location in a dedicated sitting area. Thus, passengers located surrounding the emitting antenna will be exposed to higher E-field exposure levels than users

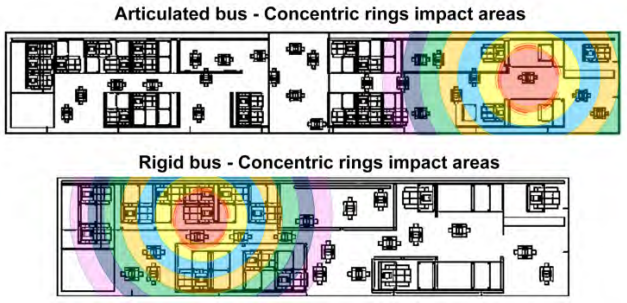

FIGURE 11. Concentric rings impact areas for the articulated and rigid buses.

TABLE 5. Comparison of E-field average values per different concentric rings impact areas and users' distribution, with the maximum allowed transmitting power.

Range Concentric Rings	Articulated Bus (F = 900 MHz) E-field average (V/m)			Rigid Bus (F = 1800 MHz) E-field average (V/m)		
	Low Dens	Med Dens	High Dens	Low Dens	Med Dens	High Dens
1m - 1.5m	NF*	NF*	NF*	8.59	8.79	9.04
1.5m - 2m	9.62	8.90	9.32	4.53	4.73	4.73
2m - 2.5m	9.94	9.78	7.83	3.25	3.27	2.96
2.5m - 3m	5.34	5.72	5.49	2.85	2.67	2.55
3m - 3.5m	5.42	4.64	4.43	2.67	2.42	2.27
3.5m - 4m	4.97	4.81	3.76	1.91	1.58	1.79

NF* = Near Field

distributed in a further distance. As expected, this phenomenon is more pronounced for the high-density cases. Moreover, it's worth noting that a higher density of passengers within the buses increases the probability of new emitting sources, expanding at the same time, the EMF exposure to other nearby passengers and consequently, multiplying the impact area.

The previous analysis reveals that dimensions, morphology and topology of the scenario, as well as human body model densities within it, highly influence radio wave propagation, leading to significant E-field exposure level variability, which must be analyzed.

B. ANALYSIS OF IMPACT AREAS

In this section, the analysis and comparison of E-field exposure levels for the different impact areas within both type of buses is presented. Low human density and the maximum transmitted power allowed per frequency band, have been considered for simulation, emulating the best EMF propagation case. Multiple transceiver locations and different frequency bands have been selected to assess accurate and relevant E-field exposure patterns. In order to provide clear insight of E-field exposure average values, results have been divided per areas along the different analyzed planes.

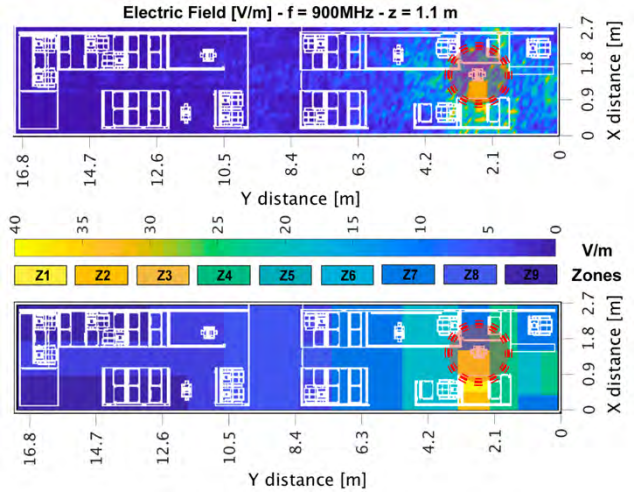

FIGURE 12. E-field exposure levels (top) and averages per areas (bottom) within the articulated bus at GSM 900. Transmitter placed in the front of the bus with the maximum allowed transmitting power. 4λ m exclusion area around the transmitter has been considered in order to avoid near field results.

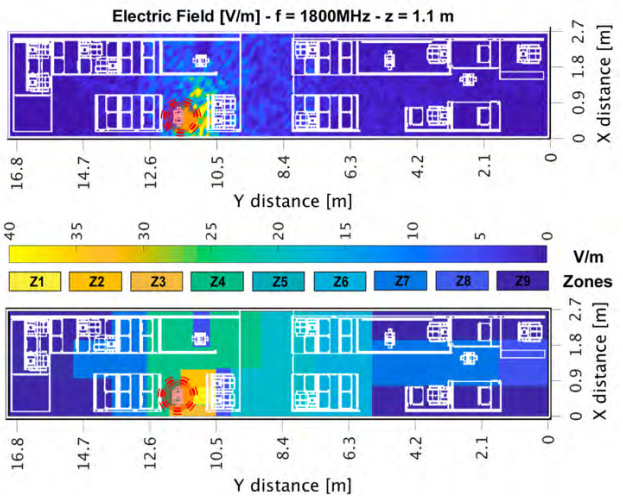

FIGURE 14. E-field exposure levels (top) and averages per areas (bottom) within the articulated bus at GSM 1800. Transmitter placed in the rear part of the bus with the maximum allowed transmitting power. 6λ m exclusion area around the transmitter has been considered in order to avoid near field results.

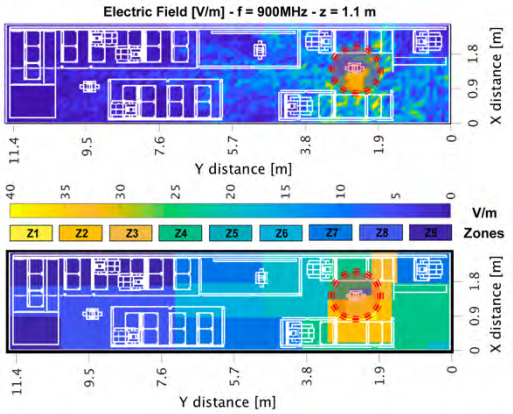

FIGURE 13. E-field exposure levels (top) and averages per areas (bottom) within the rigid bus at GSM 900. Transmitter placed in the front of the bus with the maximum allowed transmitting power. 4λ m exclusion area around the transmitter has been considered in order to avoid near field results.

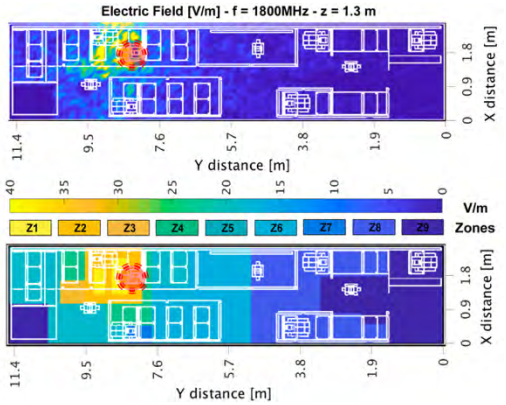

FIGURE 15. E-field exposure levels (top) and averages per areas (bottom) within the rigid bus at GSM 1800. Transmitter placed in the rear part of the bus with the maximum allowed transmitting power. 6λ m exclusion area around the transmitter has been considered in order to avoid near field results.

Fig. 12 and Fig. 13 present the E-field exposure levels at GSM 900 frequency band, for the articulated and rigid bus. For both cases and regardless the different indoor design, the transmitter location has been placed in the front part of the bus, emulating a standing person making a phone call in the center aisle. As it can be observed, E-field exposure results are clearly attenuated by body shielding created by the user who is making the phone call. In addition, the indoor open areas within the vehicles, present the most homogeneous EMF exposure distribution patterns, based on the distance to the transmitter location (E-field decreases as the transceivers distance increases). For the articulated bus case, as the length is larger than the rigid bus, it can be observed that the E-field exposure levels in the medium – rear portion of the bus are almost negligible. Both scenarios tend to a similar EMF exposure distribution pattern with no other users nearby the emitting antenna or interfering normal signal propagation.

In Fig. 14 and Fig. 15, E-field exposure comparison for both buses is presented, for the GSM 1800 frequency band. For this analysis, different transmitter locations have been placed in the rear part of the buses. In the articulated bus case, the transmitter has been placed in a semi-open delimited area, emulating a standing passenger making a phone call, while in the rigid bus, the transmitter has been placed in a dedicated sitting area emulating a sitting passenger making a phone call surrounded by other passengers. As it was expected, the E-field exposure concentration in the dedicated sitting area is significantly larger than the one in the medium open area. The E-field average distribution pattern follows a homogeneous trend in open spaces and presents large variability in delimited or dedicated areas due to multipath propagation phenomena, caused by the morphology of the scenario, indoor design

(seats, handholds, panels), user distribution, body shielding and the large amount of metal within the buses.

The EMF exposure results obtained for the bus driver critical area must be carefully analyzed. For both type of buses and configurations, E-field exposure levels in the driver location were very low (below 5V/m), even when the transmitter antenna was placed in the front part of the bus, as it can be seen in Fig. 12 and Fig. 13. It can be observed that, for all cases, these exposure results have been attenuated by the morphology of the scenario (driver delimitated area, furniture and obstacles) and the presence of nearby users. Therefore, an adequate vehicle indoor design (open spaces vs delimited and dedicated sitting areas), with a protected driver location (by means of an EMF exposure blocking wall or a closed panel), avoids high E-field hot spots within public transportation buses. In addition, a uniform passenger distribution is recommended when the bus has a high user density, in order to decrease the exposure multiplying effect and minimize the E-field exposure concentration due to body shielding.

C. ICNIRP COMPARISON WITH MAXIMUM TRANSMITTED POWER

In this section, the linear E-field exposure distribution levels, obtained within the different transportation buses, have been compared with the current ICNIRP legal EMF exposure limits. For the different frequency bands, the maximum transmitted power allowed has been considered for simulations, emulating the mobile call set-up uplink connection, which correspond with the highest device emitting power, as it is described in Table 3. Simulations have been performed with a medium value of passenger density, due to the fact that it is statistically the most probable distribution for an urban transportation business day, in terms of users per day average.

Fig. 16 presents the comparison of the articulated bus maximum E-field exposure distribution levels obtained for the different transmitter locations and frequencies analyzed. Three different transmitter locations (depicted in Fig. 6) have been considered for simulation: for the 900MHz frequency band, the transmitter has been placed in the central aisle of the vehicle's front part, for the 1800MHz frequency band, in the central part and for the 2100MHz frequency band, in a dedicated sitting area at the rear part of the bus. The obtained E-field exposure impact area, for the 900MHz frequency band, covers an area of 1.75m-2.25m radius approximately from the transmitting location due to an indoor open space location (central aisle) with less obstacles and passengers surrounding the antenna. On the other hand, for the 1800MHz and 2100MHz frequency bands, E-field results present a higher exposure concentration, with a smaller impact area delimited by 1.25m-1.5m radius respectively, from the emitting device. The transceiver locations and the involved obstacles (metallic structures, furniture and other passengers), have a relevant impact in exposure level concentration and distribution. In addition, it can be seen that E-field exposure levels for the 2100MHz frequency band present the highest

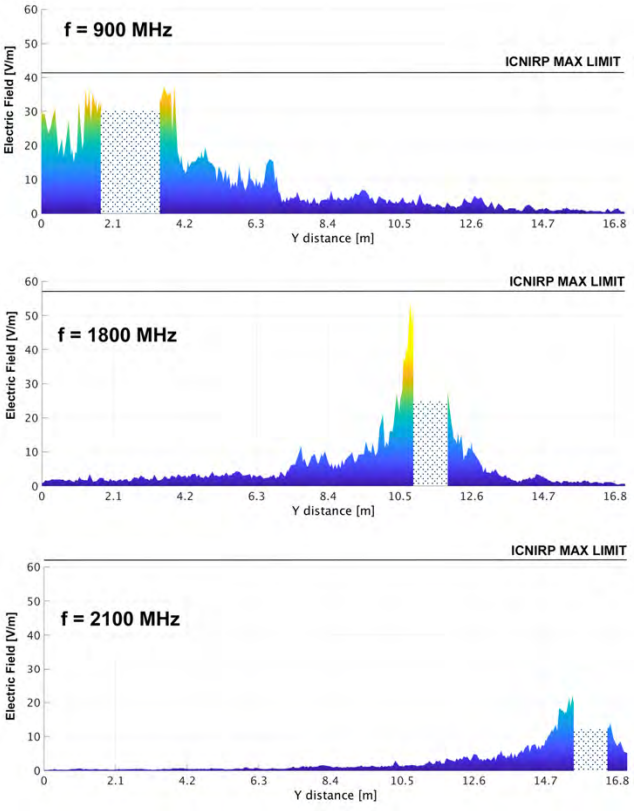

FIGURE 16. Comparison of the linear E-field exposure distribution along the articulated bus with the current ICNIRP legal limits. The corresponding exclusion areas around the transmitters have been considered in order to avoid near field results.

tolerance with the current EMF exposure limits. This is because the maximum transmitting power allowed for this frequency band, is the lowest, as it is shown in Table 3.

A similar comparison has been obtained for the rigid bus which is presented in Fig.17. In the same way, two different transmitter locations (depicted in Fig. 6) have been chosen for simulation: for the 900MHz frequency band, the transmitter has been placed at the front part of the rigid bus, in the central aisle, and for the 1800MHz, in the rear part of the vehicle, in a dedicated sitting area, where more obstacles (metallic structures, furniture and other passengers) are involved. As expected, the exposure results show a remarkable difference between open spaces and delimited dedicated spaces. Results for the 900MHz case cover a bigger exposure impact area of 1.5m-2m radius approximately from the transmitting antenna. On the other hand, a 1m-1.5m radius impact area is obtained for the 1800MHz case. In addition, and regardless of the selected frequency band, the obtained E-field exposure levels for the rigid bus case follow a more heterogeneous distribution, due to the difference in bus lengths.

Regarding legal compliance, the highest E-field exposure values are below the ICNIRP limits, considering the highest transmitted power for all cases. Moreover, for all analyzed cases, a high exposure impact area of approximately 2m is observed, where a significant attenuation decrease pattern

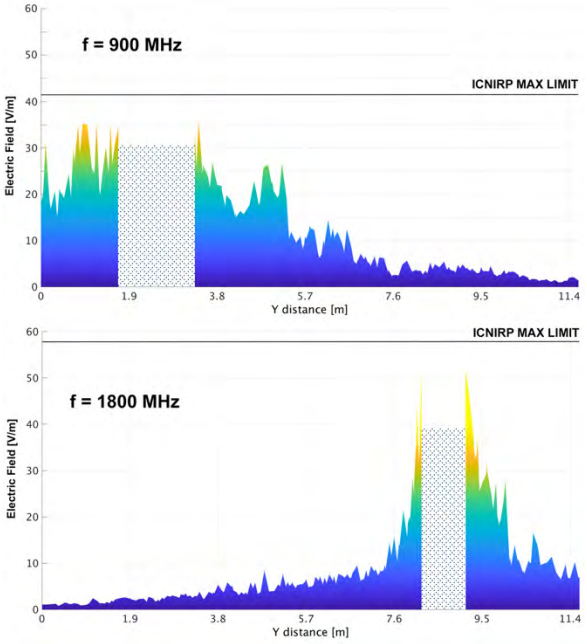

FIGURE 17. Comparison of the linear E-field exposure distribution along the rigid bus with the current ICNIRP legal limits. The corresponding exclusion areas around the transmitters have been considered in order to avoid near field results.

TABLE 6. Comparison of E-field decrease percentage per frequency for the medium human density case, at the maximum allowed transmitting power. The corresponding exclusion areas around the transmitters have been considered in order to avoid near field results.

Type of Bus Scenario	Frequency (MHz)	Maximum E-field Value (V/m) (R = 2 m)	Reference E-field Value (V/m)	Percentage E-field Decrease (%)
Articulated Bus Scenario	900	38.12	12.73	66.61
	1800	53.65	3.94	92.66
	2100	22.13	6.04	72.71
Rigid Bus Scenario	900	37.42	14.92	60.13
	1800	53.89	8.41	84.40

is presented outside this area. To gain insight in the behavior of E-field levels of this impact area and remote areas, a minimum reference E-field value (border) has been considered to compare the E-field decrease between both exposure areas. Table 6 presents the E-field decrease percentage, along with the maximum E-field level in the impact area and the minimum reference level, for all cases presented in Fig. 16 and Fig. 17. As it can be seen from the results, the lowest E-field difference is 22.5V/m, which represent a 60.13% E-field decrease for the rigid bus scenario at 900MHz frequency. On the other hand, for the articulated bus scenario, the highest E-field difference is 49.71V/m, which represent a 92.66% E-field decrease, at 1800MHz frequency.

D. MEASUREMENTS RESULTS

As previously explained in detail in Section III.A, an EMF campaign of measurements was designed and performed

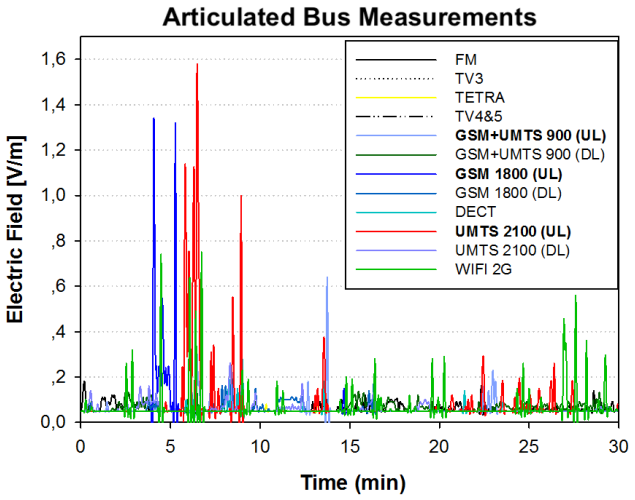

FIGURE 18. Measurement results within the articulated bus along the Line 6 route, by means of EME Spy 121 personal dosimeter.

within different types of public buses, along real transportation routes of the city of Pamplona. In Fig. 18 and Fig. 19, the E-field PEM's measurement results for two different routes are depicted. The measured EMF exposure levels within the different kind of buses are extremely low (below 3V/m). For all cases the highest E-field levels are produced by mobile communication systems (GSM/UMTS), initiated by the mobile voice connections during the measurement campaign. In Fig. 18, the highest E-field exposure values correspond with the different transmitter locations within the articulated bus (i.e. the exposure values in the GSM 900 frequency band correspond with the first transmitter location in the front part of the bus, the values in GSM 1800 with the second transmitter location in the central part of the bus and the highest values in UMTS 2100 are linked to the third transmitter location in the rear part of the bus). In the same way, the highest E-field exposure values correspond with the different transmitter locations within the rigid bus. It's worth noting that the PEM measurements can be affected by the presence of passengers within the analyzed scenarios [50] and the selected measurement procedure and locations. The E-field exposure values measured using PEM devices, tend to underestimate true exposure levels by about a factor of two due to shielding effects of the human body, as it has been presented in [51]. Hence, the reliability and accuracy of the PEM measurements must be analyzed carefully. To reduce or avoid underestimation, measurements were performed with the PEM in the vicinity of the body, but not directly on the body. Following this approach, the highest E-field exposure level (2.8V/m) correspond with the transmitter placed at the bottom of the rigid bus. Therefore, the presented exposure levels verify compliance with current EMF legal exposure limits (56V/m allowed by the ICNIRP).

As in the real measurements, the same transmitter locations have been considered in the simulations to compare the obtained results with the measured ones. For that purpose,

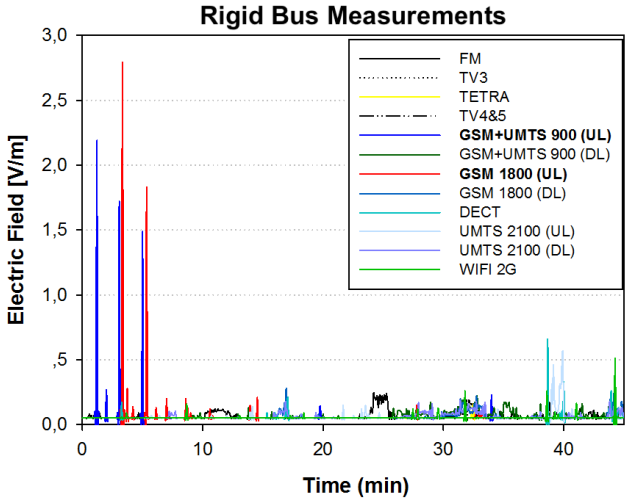

FIGURE 19. Measurement results within the rigid bus along the Line 4 route, by means of EME Spy 121 personal dosimeter.

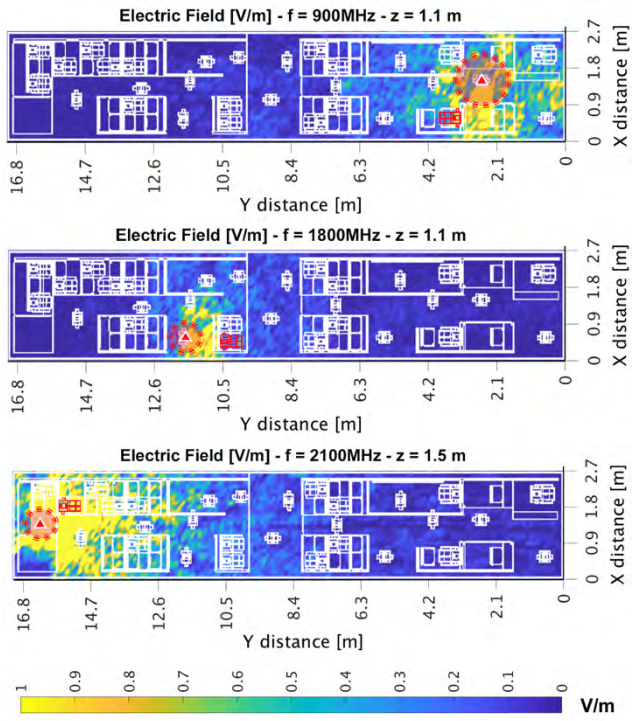

FIGURE 20. E-field exposure levels within the articulated bus for different frequencies and transmitter locations, at the minimum allowed transmitting power. The corresponding exclusion areas around the transmitters have been considered in order to avoid near field results.

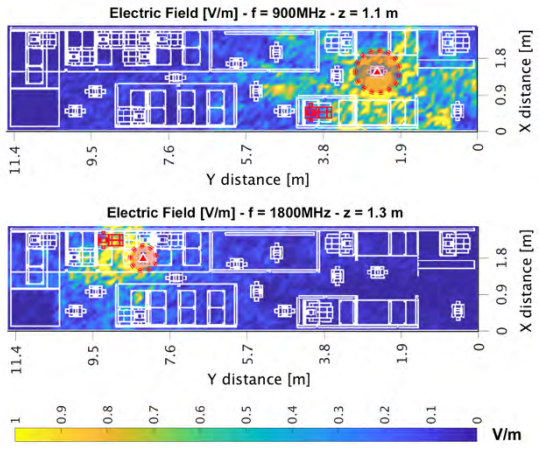

FIGURE 21. E-field exposure levels within the rigid bus for different frequencies and transmitter locations, at the minimum allowed transmitting power. The corresponding exclusion areas around the transmitters have been considered in order to avoid near field results.

TABLE 7. Comparison of EMF exposure levels for users' different body areas, considering a medium human density simulation case with the minimum allowed transmitting power. The analyzed user is represented as the red colored passenger in Fig 16 - 17.

		Chest (Rx) E-field (V/m)		Head (Rx) E-field (V/m)	
Type of Bus Scenario	Freq (MHz)	Min Power	Max Power	Min Power	Max Power
Articulated Bus scenario	900	0.37	6.15	0.87	16.87
	1800	0.18	18.20	0.81	25.87
	2100	1.15	5.76	1.30	17.11
Rigid Bus Scenario	900	0.45	11.24	0.47	14.79
	1800	1.46	26.09	1.49	30.24

the minimum transmitted power was considered (see Table 3), emulating the best transmission uplink case, as the specific transmission power of the mobile phone during the calls was unknown. In Fig. 20 and Fig. 21, simulated EMF exposure levels are presented for the different frequency bands assessed. Notice that the scale used in these figures has a maximum of 1V/m instead of the previous 40V/m scale shown in previous sections, when considering the maximum transmitted power. The transmitter position is represented with a red and white triangle and measurements were performed in the closest available sitting location within an action area radius of 2m, depicted with a red passenger in the figures (PEM location).

As it was expected, for all the analyzed results, the PEMs EMF exposure values are lower than those from the real measurements because simulations were performed with the best transmitted power set up. As Fig. 20 presents, the articulated bus measurements were affected by body shielding due to the bus indoor morphology design which allows a confronted passenger's location between the emitting source and the PEM. As stated above, to minimize or prevent this shielding effect, which can reduce measurement values significantly [52], [53], the PEM was located in the vicinity of the body, not on the body. Thus, as it can be observed in Fig. 18 and Fig. 19, this procedure reduced in approximately 1V/m the differences between the PEM measurements of the articulated bus versus the rigid bus measurements, which were not affected by body shielding.

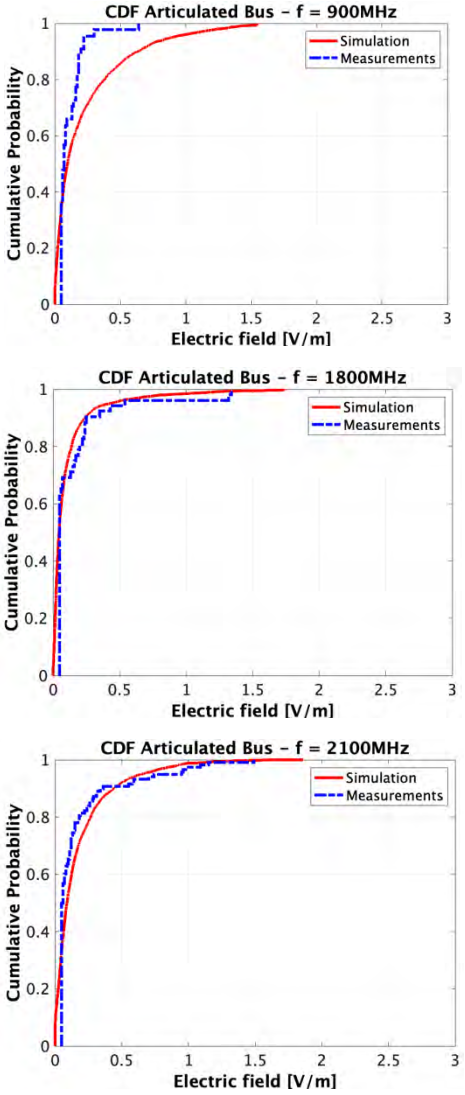

FIGURE 22. CDF of simulation and measurement values within the articulated bus for different frequencies.

To have clear insight into the comparison between simulation and measurements, the cumulative distribution functions (CDFs) have been obtained and are presented in Fig. 22 and Fig. 23, for the articulated and rigid bus respectively. It can be seen that simulation results are in accordance with measurements, with 90% approximately of the measured and simulated values below 0.5V/m for all cases.

In Table 7, a comparison of simulated EMF exposure levels in different body areas (chest and head) is presented. As it was expected, simulation results show huge differences in estimated E-field exposure values depending on the transmission power (maximum transmitted power vs minimum transmitted power). For all cases, passenger heads are more exposed to non-ionizing radiation, but it can be remarked that the obtained EMF exposure levels are low in comparison with the ICNIRP limits.

Therefore, the comparison with current legal exposure limits has been presented, verifying that, for all cases,

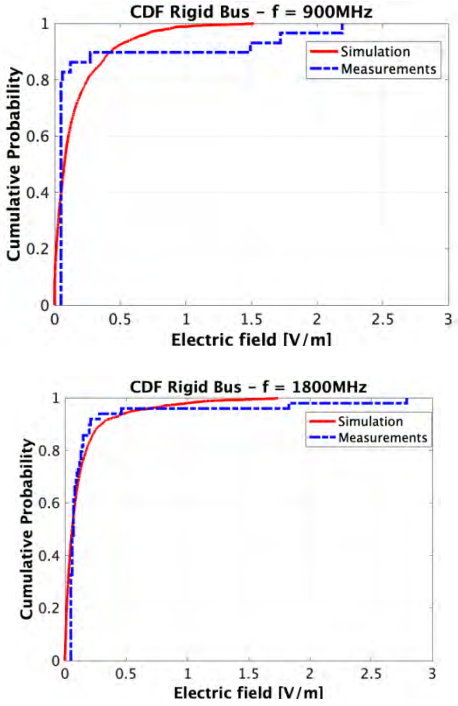

FIGURE 23. CDF of simulation and measurement values within the rigid bus for different frequencies.

E-field levels were below the aforementioned limits. These results and the proposed simulation methodology, can aid in an adequate assessment of EMF exposure recommendations and limits, for current and future wireless communication systems, in urban transportation buses.

V. CONCLUSIONS

This work presents a complete E-field strength distribution spatial characterization for different types of urban transportation buses. E-field exposure level estimations have been obtained by means of an in-house developed deterministic 3D-RL algorithm, for the complete indoor volume of the transportation buses. By using this methodology, the impact of topology, dimensions and morphology as well as materials, body shielding and user distribution, has been considered with an effective and efficient balance between accuracy and computational cost. For both type of public buses, EMF exposure level measurements have been performed, by means of a PEM, along the analyzed routes for different scenarios setups, verifying compliance with the current international legal exposure benchmark limits. A validated measurement procedure has been followed, with the PEM located in the vicinity of the body, not on the body, decreasing body shielding effect (only 1V/m when a confronted passenger's location is between the emitting source and the receiver) and achieving accordance between measurements and simulation results.

The presented simulation results confirm the large influence of user presence within the scenarios due to their body shielding effect and the corresponding exposure concentration in the transmitter vicinity. User E-field exposure levels

increase in the vicinity of the emitting antenna, being much more pronounced for the high-density cases within the buses. For these sensitive setups, a uniform passenger distribution is recommended to decrease the probability of new emitting sources and the undesirable exposure multiplying effect. The indoor design (dimensions, morphology and topology of the scenario) has a relevant influence in EMF exposure distribution results. A homogeneous E-field exposure distribution is obtained for open spaces, while highly variable distribution patterns are presented for delimited and dedicated areas, due mainly to multipath propagation.

The results reveal the complexity of EMF exposure characterization in this type of vehicular scenarios, due to the significant impact of multipath propagation. These results and the proposed simulation methodology are an appropriate approach to adequately assess EMF exposure recommendations and limits, for current and future wireless communication systems in urban transportation buses.

REFERENCES

[1] Eurostat, Luxembourg. (2017). *Passenger Transport Statistics*. [Online]. Available: http://ec.europa.eu/eurostat/statistics-explained/index.php/Passenger_transport_statistics

[2] W. Xiang, Y. Huang, and S. Majhi, "The design of a wireless access for vehicular environment (WAVE) prototype for intelligent transportation system (ITS) and vehicular infrastructure integration (VII)," in *Proc. IEEE 68th Veh. Technol. Conf.*, Sep. 2008, pp. 1–2.

[3] R. P. S. Padmanaban, L. Vanajakshi, and S. C. Subramanian, "Estimation of bus travel time incorporating dwell time for APTS applications," in *Proc. IEEE Intell. Veh. Symp.*, Jun. 2009, pp. 955–959.

[4] L. Azpilicueta *et al.*, "Characterization of wireless channel impact on wireless sensor network performance in public transportation buses," *IEEE Trans. Intell. Transp. Syst.*, vol. 16, no. 6, pp. 3280–3293, Dec. 2015.

[5] World Health Organization. (May 2006). *Fact Sheet 304 Base Stations and Wireless Technology*. [Online]. Available: http://www.who.int/peh-emf/publications/factsheets/en/

[6] S. Aerts, D. Plets, A. Thielens, L. Martens, and W. Joseph, "Impact of a small cell on the RF-EMF exposure in a train," *Int. J. Environ. Res. Public Health*, vol. 12, no. 3, pp. 2639–2652, 2015.

[7] E. Aguirre *et al.*, "Analysis of estimation of electromagnetic dosimetric values from non-ionizing radiofrequency fields in conventional road vehicle environments," *Electromagn. Biol. Med.*, vol. 34, no. 1, pp. 19–28, 2015.

[8] E. Aguirre *et al.*, "Estimation of electromagnetic dosimetric values from non-ionizing radiofrequency fields in an indoor commercial airplane environment," *Electromagn. Biol. Med.*, vol. 33, no. 4, pp. 252–263, 2014.

[9] K. Gryz and J. Karpowicz, "Radiofrequency electromagnetic radiation exposure inside the metro tube infrastructure in Warszawa," *Electromagn. Biol. Med.*, vol. 4, no. 3, pp. 265–273, 2015.

[10] D. Plets *et al.*, "Assessment of contribution of other users to own total whole-body RF absorption in train environment," *Bioelectromagnetics*, vol. 36, no. 8, pp. 597–602, 2015.

[11] C. Visvikis, "Safety considerations for electric vehicles and regulatory activities," in *Proc. 26th Int. Battery, Hybrid Fuel Cell Electr. Vehicle Symp.*, 2012, pp. 1–14.

[12] M. N. Halgamuge, C. D. Abeyrathne, and P. Mendis, "Measurement and analysis of electromagnetic fields from trams, trains and hybrid cars," *Radiat. Protection Dosimetry*, vol. 141, pp. 255–268, Jun. 2010.

[13] *On the Limitation of Exposure of the General Public to Electromagnetic Fields (0 Hz to 300 GHz)*, document 1999/519/EC, EUROPEAN Council Recommendation, 1999.

[14] International Commission on Non-Ionizing Radiation Protection, "Guidelines for limiting exposure to time-varying electric, magnetic, and electromagnetic fields (up to 300 GHz)," *Health Phys.*, vol. 74, no. 4, pp. 494–522, 1998.

[15] *Model Legislation for Electromagnetic Fields Protection*, World Health Org., Geneva, Switzerland, 2006. [Online]. Available: http://www.who.int/peh-emf/standards/EMF_model_legislation[1].pdf

[16] S. Valbonesi, C. Carciofi, and B. Bisceglia, "Precautionary principle application and 5G development," in *Proc. IEEE 29th Annu. Int. Symp. Pers., Indoor, Mobile Radio Commun. (PIMRC)*, Sep. 2018, pp. 1192–1196.

[17] *Guidelines on the Application of the Precautionary Principle*, Eur. Commission, Brussels, Belgium, 1988.

[18] *Communication From the Commission on the Precautionary Principle*, Eur. Commission, Brussels, Belgium, 2000.

[19] C. R. Roy and L. J. Martin, "A comparison of important international and national standards for limiting exposure to EMF including the scientific rationale," *Health Phys.*, vol. 92, no. 6, pp. 635–641, 2007.

[20] *Limits of Human Exposure to Radiofrequency Electromagnetic Energy in the Frequency Range from 3 KHz to 300 GHz*, Healthy Environ. Consum. Saf. Branch, Ottawa, ON, Canada, 2009. [Online]. Available: http://www.rfsafetysolutions.com/RF%20Radiation%20Pages/Safety_Code_6.html

[21] *Specific Absorption Rate (SAR) for Cellular Telephones*, Federal Commun. Commission, Washington, DC, USA, 2011. [Online]. Available: http://www.fcc.gov/encyclopedia/specific-absorption-rate-sar-cellular-telephones

[22] National Institute for Public Health and the Environment, Bilthoven, The Netherlands. (Jan. 2018). *Comparison of International Policies on Electromagnetic Fields (Power Frequency and Radiofrequency Fields)*. [Online]. Available: https://www.rivm.nl/sites/default/files/2018-11/Comparison%20of%20international%20policies%20on%20electromagnetic%20fields%202018.pdf

[23] *IEEE Recommended Practice for Radio Frequency Safety Programs, 3 KHz to 300 GHz*, IEEE Standard C95.7, Mar. 2006, pp. 1–52.

[24] P. Gajsek, A. G. Pakhomov, and B. J. Klauenberg, "Electromagnetic field standards in central and eastern European countries: Current state and stipulations for international harmonization," *Health Phys.*, vol. 82, no. 4, pp. 473–483, 2002.

[25] J. M. Osepchuk and R. C. Petersen, "Historical review of RF exposure standards and the international committee on electromagnetic safety (ICES)," *Bioelectromagnetics*, vol. 6, pp. S7–S16, 2003.

[26] M. Repacholi, Y. Grigoriev, J. Bushmann, and C. Pioli, "Scientific basis for the soviet and Russian radiofrequency standards for the general public," *Bioeletromagnetics*, vol. 33, no. 8, pp. 623–633, 2012.

[27] Radiofrequency Radiation. (2013). *ARPANSA—Australian Radiation Protection and Nuclear Safety Agency*. [Online]. Available: http://www.arpansa.gov.au/radiationprotection/basics/rf.cfm

[28] *BOE-A-2001-18256, Spain*. Accessed: 2011. [Online]. Available: https://www.boe.es/eli/es/rd/2001/09/28/1066/con

[29] *Amending Directive 2004/40/EC on Minimum Health and Safety Requirements Regarding the Exposure of Workers to the Risks Arising from Physical Agents (Electromagnetic Fields) (18th Individual Directive within the Meaning of Article 16(1) of Directive 89/391/EEC)*, Eur. Parliament, Brussels, Belgium, 2013.

[30] J. F. Bolte, M. Maslanyj, D. Addison, T. Mee, J. Kamer, and L. Colussi, "Do car-mounted mobile measurements used for radio-frequency spectrum regulation have an application for exposure assessments in epidemiological studies?" *Environ. Int.*, vol. 86, pp. 75–83, Jan. 2016.

[31] J. González-Rubio, A. Nájera, and E. Arribas, "Comprehensive personal RF-EMF exposure map and its potential use in epidemiological studies," *Environ. Res.*, vol. 149, pp. 105–112, Aug. 2016.

[32] D. Urbinello, A. Huss, J. Beekhuizen, R. Vermeulen, and M. Röösli, "Use of portable exposure meters for comparing mobile phone base station radiation in different types of areas in the cities of Basel and Amsterdam," *Sci. Total Environ.*, vol. 48, pp. 1028–1033, Jan. 2014.

[33] J. Isabona and V. M. Srivastava, "Cellular mobile phone—A technical assessment on electromagnetic radiation intensity on human safety," in *Proc. IEEE 3rd Int. Conf. Electro-Technol. Nat. Develop. (NIGERCON)*, Nov. 2017, pp. 271–274.

[34] L. Azpilicueta, M. Rawat, K. Rawat, F. Ghannouchi, and F. Falcone, "A ray launching-neural network approach for radio wave propagation analysis in complex indoor environments," *IEEE Trans. Antennas Propag.*, vol. 62, no. 5, pp. 2777–2786, May 2014.

[35] E. Aguirre, P. López-Iturri, L. Azpilicueta, J. Arpón, and F. Falcone, "Characterization and consideration of topological impact of wireless propagation in a commercial aircraft environment," *IEEE Antennas Propag. Mag.*, vol. 55, no. 6, pp. 240–258, Dec. 2013.

[36] P. López-Iturri, E. Aguirre, L. Azpilicueta, U. Gárate, and F. Falcone, "ZigBee radio channel analysis in a complex vehicular environment," *IEEE Antennas Propag. Mag.*, vol. 56, no. 4, pp. 232–245, Aug. 2014.
[37] A. Skrebtsov, A. Burnic, D. Xu, A. Waadt, and P. Jung, "UWB applications in public transport," in *Proc. Int. Conf. CCCA*, Hammamet, Tunisia, Mar. 2011, pp. 1–4.
[38] F. Bellens, F. Quitin, F. Horlin, and P. De Doncker, "Channel measurements and MB-OFDM performance inside a driving car," in *Proc. Int. Conf. Electromagn. Adv. Appl.*, Torino, Italy, Sep. 2009, pp. 392–395.
[39] N. Alam and A. G. Dempster, "Cooperative positioning for vehicular networks: Facts and future," *IEEE Trans. Intell. Transp. Syst.*, vol. 14, no. 4, pp. 1708–1717, Dec. 2013.
[40] J. Zhou, C. L. P. Chen, L. Chen, and W. Zhao, "A user-customizable urban traffic information collection method based on wireless sensor networks," *IEEE Trans. Intell. Transp. Syst.*, vol. 14, no. 3, pp. 1119–1128, Sep. 2013.
[41] M. F. Iskander and Z. Yun, "Propagation prediction models for wireless communication systems," *IEEE Trans. Microw. Theory Techn.*, vol. 50, no. 3, pp. 662–673, Mar. 2002.
[42] J.-P. Rossi and Y. Gabillet, "A mixed ray launching/tracing method for full 3-D UHF propagation modeling and comparison with wide-band measurements," *IEEE Trans. Antennas Propag.*, vol. 50, no. 4, pp. 517–523, Apr. 2002.
[43] V. Degli-Esposti *et al.*, "Efficient RF coverage prediction through a fully discrete, GPU-parallelized ray-launching model," in *Proc. 12th Eur. Conf. Antennas Propag. (EuCAP)*, London, U.K., 2018, pp. 220–225.
[44] Z. Lai, "Intelligent ray launching algorithm for indoor scenarios," *Radioengineering*, vol. 20, no. 2, pp. 1–11, Jun. 2011.
[45] L. Azpilicueta, M. Rawat, K. Rawat, F. Ghannouchi, and F. Falcone, "Convergence analysis in deterministic 3D ray launching radio channel estimation in complex environments," *ACES J.*, vol. 29, no. 4, pp. 256–271, 2014.
[46] S. Salous, *Radio Propagation Measurement and Channel Modelling*. Hoboken, NJ, USA: Wiley, 2013.
[47] E. Aguirre, J. Arpon, L. Azpilicueta, S. De Miguel Bilbao, V. Ramos, and F. Falcone, "Evaluation of electromagnetic dosimetry of wireless systems in complex indoor scenarios with human body interaction," *Prog. Electromagn. Res. B*, vol. 43, pp. 189–209, Aug. 2012.
[48] L. Azpilicueta, F. Falcone, and R. Janaswamy, "A hybrid ray launching-diffusion equation approach for propagation prediction in complex indoor environments," *IEEE Antennas Wireless Propag. Lett.*, vol. 16, pp. 214–217, May 2016.
[49] L. Azpilicueta, P. López-Iturri, E. Aguirre, C. Vargas-Rosales, A. León, and F. Falcone, "Influence of meshing adaption in convergence performance of deterministic ray launching estimation in indoor scenarios," *J. Electromagn. Waves Appl.*, vol. 31, no. 5, pp. 544–559, 2017.
[50] U. Knafl, H. Lehmann, and M. Riederer, "Electromagnetic field measurements using personal exposimeters," *Bioelectromagnetics*, vol. 29, no. 2, pp. 160–162, 2008.
[51] G. Neubauer, S. Cecil, W. Giczi, B. Petric, P. Preiner, J. Frohlich, "Final report on the project C2006-07, evaluation of the correlation between RF dosimeter reading and real human exposure," ETH Zürich, Zürich, Switzerland, Tech. Rep. ARC-IT-0218, Apr. 2008.
[52] J. Blas, F. A. Lago, P. Fernandez, R. M. Lorenzo, and E. J. Abril, "Potential exposure assessment errors associated with body-worn RF dosimeters," *Bioelectromagnetics*, vol. 28, no. 7, pp. 573–576, 2007.
[53] S. Iskra, R. McKenzie, and I. Cosic, "Factors influencing uncertainty in measurement of electric fields close to the body in personal RF dosimetry," *Radiat. Protection Dosimetry* vol. 140, no. 1, pp. 25–33, 2010.

MIKEL CELAYA-ECHARRI (S'18) received the Computer Science Engineering degree and the M.Sc. degree in project management from the Public University of Navarre, Pamplona, Navarre, in 2011 and 2015, respectively. From 2011 to 2014, he was a Research and Development Engineer with Tafco Metawireless, Spain. From 2015 to 2017, he was a Visiting Assistant with the Networks and Telecommunications Research Group, Tecnologico de Monterrey. He is currently pursuing the Ph.D. degree in engineering of science with the Tecnologico de Monterrey, Mexico. His research interests include high-frequency electromagnetic dosimetry, radio frequency propagation, wireless sensor networks, project management, and computer science.

LEYRE AZPILICUETA (M'15) received the Telecommunications Engineering degree, the master's degree in communications, and the Ph.D. degree in telecommunication technologies from the Public University of Navarre, in Spain, in 2009, 2011, and 2015, respectively. In 2010, she was with the Research and Development Department of RFID Osés as a Radio Engineer. She is currently an Associate Professor and a Researcher with the Tecnologico de Monterrey, Campus Monterrey, Mexico. Her research interests include radio propagation, mobile radio systems, ray tracing, and channel modeling. She has over 150 contributions in relevant journals and conference publications. She was a recipient of the IEEE Antennas and Propagation Society Doctoral Research Award 2014, the Young Professors and Researchers Santander Universities 2014 Mobility Award, the ECSA 2014 Best Paper Award, the IISA 2015 Best Paper Award, the best Ph.D. in 2016 awarded by the Colegio Oficial de Ingenieros de Telecomunicación, and the N2Women: Rising Stars in Computer Networking and Communications' 2018 Award.

PEIO LOPEZ-ITURRI (M'16) received the Telecommunications Engineering degree, the master's degree in communications, and the Ph.D. degree in communication engineering from the Public University of Navarre, Pamplona, Navarre, in 2011, 2012, and 2017, respectively. He gets the 2018 Best Spanish Ph.D. thesis in Smart Cities in CAEPIA 2018 (third prize), sponsored by the Spanish network on research for Smart Cities CI-RTI and Sensors (ISSN 1424-8220). He has worked in ten different public and privately funded research projects. He has over 120 contributions in indexed international journals, book chapters, and conference contributions. He is also affiliated with the Institute for Smart Cities, UPNA. His research interests include radio propagation, wireless sensor networks, electromagnetic dosimetry, modeling of radio interference sources, mobile radio systems, wireless power transfer, the IoT networks and devices, 5G communication systems, and EMI/EMC. He has been awarded the ECSA 2014 Best Paper Award and the IISA 2015 Best Paper Award.

ERIK AGUIRRE received the M.Sc. degree in telecommunications engineering from the Public University of Navarre, in 2012, and the Ph.D. degree in 2014. From 2012 to 2014, he worked in a research project at the University of Vigo related to dispersive propagation. Since 2015, he has been with Tafco Metawireless. Since 2016, he has been an Assistant Lecturer with UPNA. His research interests include radio propagation in dispersive media, body centric communications, and wireless sensor networks.

SILVIA DE MIGUEL-BILBAO received the Telecommunication Engineering and Ph.D. degrees from the University of Valladolid (UVA), Spain, in 2001 and 2015, respectively. From 2000 to 2009, she was a Research and Development Engineer in the private industry, and from 2005 to 2009, she was also an Associate Lecturer with UVA. Since 2010, she has been a Researcher in the Research Area of Telemedicine and e-Health with the Carlos III Health Institute. Her main research interests include experimental and numerical dosimetry in bio-electromagnetics, electromagnetic compatibility, smart health, radio-frequency electromagnetic fields, as well as the assessment of exposure to non-ionizing radiations. She has authored or co-authored numerous journal and conference papers with impact factor as well as book chapters. She was a recipient of the Doctorate Award 2016 in the engineering and architecture area awarded by UVA.

VICTORIA RAMOS (SM'15) received the Telecommunications Engineer degree from the Polytechnic University of Madrid, Madrid, Spain, and the Ph.D. degree in biomedical engineering and telemedicine from the University of Alcala, Madrid, in 2005. From 1985 to 1996, she was a Radio Communications Research and Development Engineer in the private industry. Since 1996, she has been a Research Scientist and now she is a Ph.D. Researcher, as a Civil Servant, at the Health Institute Carlos III, belonging to the Ministry of Science, Innovation and University, in the Research Area of Telemedicine and e-Health, Madrid. Her research focuses on the area of wireless communications applications for home care and the next generations of sensors networks and body area networks and telemedicine applications. The objectives are to provide health care for mobile citizens and e-Health focusing on new emergent health services based on telemedicine. It involves standards related to human exposure, medical devices immunity, and radio communication EMC. She has authored or co-authored several books as well as several papers for scientific congresses. She takes part in several European and Spanish research projects and European and Spanish Standardizations Committees.

FRANCISCO FALCONE (M'05–SM'09) received the Telecommunication Engineering degree and the Ph.D. degree in communication engineering from the Universidad Pública de Navarra (UPNA), Spain, in 1999 and 2005, respectively. From 1999 to 2000, he was a Microwave Commissioning Engineer with Siemens-Italtel, deploying microwave access systems. From 2000 to 2008, he was a Radio Access Engineer with Telefónica Móviles, performing radio network planning and optimization tasks in mobile network deployment. In 2009, as a Co-Founding Member, he was the Director of Tafco Metawireless, a spin-off company from UPNA. In parallel, he was an Assistant Lecturer with the Electrical and Electronic Engineering Department, UPNA, from 2003 to 2009. In 2009, he became an Associate Professor with the EE Department and then the Department Head, from 2012 to 2018. In 2018, he was a Visiting Professor with the Kuwait College of Science and Technology, Kuwait. He is also affiliated with the Institute for Smart Cities, UPNA, which hosts around 140 researchers, currently acting as the Head of the ICT section. His research interests include computational electromagnetics applied to the analysis of complex electromagnetic scenarios with a focus on the analysis, design, and implementation of heterogeneous wireless networks to enable context-aware environments. He has over 500 contributions in indexed international journals, book chapters, and conference contributions. He has been awarded the CST 2003 and CST 2005 Best Paper Award, the Ph.D. Award from the Colegio Oficial de Ingenieros de Telecomunicación, in 2006, the Doctoral Award UPNA, in 2010, the First Juan Gomez Peñalver Research Award from the Royal Academy of Engineering of Spain, in 2010, the XII Talgo Innovation Award 2012, the IEEE 2014 Best Paper Award, in 2014, the ECSA-3 Best Paper Award, in 2016, and the ECSA-4 Best Paper Award, in 2017.